Reorientation of icy satellites by impact basins

F. Nimmo[1] and I. Matsuyama[2]

Received 29 May 2007; revised 25 June 2007; accepted 5 July 2007; published 3 October 2007.

[1] Large impact basins are present on many of the icy satellites of the outer solar system. Assuming that their present-day topography is uncompensated, such basins can cause significant poleward reorientations for slow-rotating satellites. This reorientation may have been accompanied by transient large-amplitude wobble. The largest basins on Tethys, Rhea and Titania are predicted to have caused reorientations of roughly 4°, 7° and 12°, respectively, resulting in global tectonic stresses up to ~0.5 MPa. The potential anomalies associated with the basins can be up to one-third of those expected for a hydrostatic, tidally- and rotationally-deformed body, and may complicate interpretation of the satellite interior structure. Pluto and Charon, because of their slow rotation, are also likely to have undergone reorientation of 10–20° if they possess impact basins of comparable sizes to those of the Saturnian satellites.
Citation: Nimmo, F., and I. Matsuyama (2007), Reorientation of icy satellites by impact basins, *Geophys. Res. Lett.*, *34*, L19203, doi:10.1029/2007GL030798.

1. Introduction

[2] It has been recognized for half a century that the application of loads to solid planetary bodies can cause large-scale bodily reorientations with respect to the rotation axis [*Gold*, 1955]. Such reorientations lead to stresses sufficient to cause fracture, and are thus potentially recognizable in the geological record [*Melosh*, 1980]. Large (90°) reorientations have been inferred on the Earth based on paleomagnetic records [*Kirschvink et al.*, 1997]. The growth of the Tharsis Rise on Mars may also have caused significant reorientation [*Melosh*, 1980; *Willemann*, 1984].

[3] Less attention has been paid to reorientation of the icy satellites of the outer solar system. *Rubincam* [2003] investigated how redistribution of volatiles might affect the rotational stability of Triton and Pluto. *Janes and Melosh* [1988] and *Nimmo and Pappalardo* [2006] modelled reorientation due to convective processes on Miranda and Enceladus, respectively, and *Ojakangas and Stevenson* [1989] pointed out that Europa's variable ice shell thickness might lead to rotational instability. Here we will focus on the fact, first pointed out by *Melosh* [1975], that the negative long-term load caused by a large impact basin can potentially reorient a planetary body. While this mechanism has been investigated for Ganymede [*Murchie and Head*, 1986], a general survey of the kind presented here has not been carried out.

[4] The rest of this paper is organized as follows. Section 2 will outline the theory, which is based on I. Matsuyama and F. Nimmo (Rotational stability of planetary bodies with elastic lithospheres and tidal deformation, submitted to *Journal of Geophysical Research*, 2007, hereinafter referred to as Matsuyama and Nimmo, submitted manuscript, 2007) and incorporates both the tidal and rotational deformation of synchronous satellites. Section 3 will briefly discuss the pertinent observations. Sections 4 and 5 present the results of applying the theory to a variety of outer solar system bodies, and the final section discusses some consequences of these results.

2. Theory

[5] If a topographic depression is produced on a satellite, by an impact or some other means, then the moment of inertia of the body is affected [*Melosh*, 1975]. Over the long term the satellite's rotation axis will reorient to become parallel to the new axis of maximum inertia [*Matsuyama et al.*, 2006]. The reorientation will be opposed by those ("fossil") parts of the rotational and tidal bulges which are maintained elastically and do not adjust as the reorientation proceeds [*Willemann*, 1984]. A single topographic depression will always be reoriented towards the nearest pole.

[6] Our analysis is simplified because it neglects the time-dependent relaxation of the depression and the rotational bulge. Since the timescales of bulge relaxation and load relaxation are likely to be similar to each other, a full analysis including the time-dependent inertia tensor will be complicated and beyond the scope of the present work [cf. *Spada et al.*, 1996].

[7] We will consider the specific case of a tidally-deformed satellite which has no initial rigidity, and is thus purely hydrostatic. As the satellite cools, it will develop a rigid lithosphere while retaining the hydrostatic shape. At some point in the cooling process, the impact basin forms and reorientation, opposed by the fossil tidal and rotational bulges, will take place. Because of these bulges, the angular reorientation θ_R depends on the final colatitude θ_L^f and longitude ϕ_L^f of the applied load. By diagonalizing the resulting moment of inertia tensor, the following set of equations may be derived (Matsuyama and Nimmo, submitted manuscript, 2007):

$$Q \sin^2\theta_L^f \sin\left(2\phi_L^f\right) = \sin^2\theta_R \sin(2\phi_R) - 3\sin^2\theta_T \sin(2\phi_T) \quad (1)$$

$$Q \sin\left(2\theta_L^f\right) \cos\left(\phi_L^f\right) = \sin(2\theta_R)\cos(\phi_R) - 3\sin(2\theta_T)\cos(\phi_T) \quad (2)$$

[1]Department of Earth and Planetary Sciences, University of California, Santa Cruz, California, USA.
[2]Department of Terrestrial Magnetism, Carnegie Institution of Washington, Washington, D.C., USA.

0094-8276/07/2007GL030798$05.00

$$Q\sin\left(2\theta_L^f\right)\sin\left(\phi_L^f\right) = \sin(2\theta_R)\sin(\phi_R) - 3\sin(2\theta_T)\sin(\phi_T) \quad (3)$$

Here (θ_R, ϕ_R) and (θ_T, ϕ_T) are the coordinates of the initial rotational and tidal axes, respectively, and Q defines the size of the load (see below). These equations are valid in a reference frame with the x and z axes directed along the final tidal and rotational axes, respectively. The initial tidal and rotational axes must be perpendicular, and the reorientation angle is given by θ_R.

[8] For reorientation along the meridian passing through the tidal axis, these equations simplify to give $Q\sin(2\theta_L^f) = 4\sin(2\theta_R)$ while for reorientation along the meridian perpendicular to the tidal axis we obtain $Q\sin(2\theta_L^f) = \sin(2\theta_R)$ (Matsuyama and Nimmo, submitted manuscript, 2007). Thus, reorientation is larger if it occurs around the tidal axis, as expected [*Nimmo and Pappalardo*, 2006]. Equations (1)–(3) neglect the role of dissipation due to reorientation, which may be significant in some situations [*Ojakangas and Stevenson*, 1989; I. Matsuyama et al., Reorientation of planets with lithospheres: The effect of elastic energy, submitted to *Icarus*, 2007].

[9] The quantity Q describes the size of the load, and is given by (Matsuyama and Nimmo, submitted manuscript, 2007)

$$Q = \frac{GM}{R^2}\frac{3\sqrt{5}G_{20}'^L}{R\Omega^2\left(k_f^T* - k_f^T\right)} \quad (4)$$

Here R, M and Ω are the satellite radius, mass and angular rotation frequency, G is the gravitational constant, $G_{20}{}'^L$ is the dimensionless degree-two gravitational potential for the load positioned at the north pole. The quantities k_f^T* and k_f^T are the secular tidal Love numbers of the body without and with an elastic lithosphere, respectively; the difference between them defines the size of the fossil rotational bulge. Note that here we have assumed that the rotation rate is unaffected by the reorientation.

[10] To calculate the gravitational potential anomaly imposed by an impact basin we use the present-day observed depth h and assume that the basin is uncompensated; that is, all viscous stresses have relaxed and the remaining topography is elastically supported. For a pole-centred uncompensated basin having an angular radius ψ and a constant depth h, the normalized degree-2 potential when $h \ll R$ is given by

$$G_{20}'^L = \frac{\pi h\rho R^2}{\sqrt{5}M}\cos\psi\sin^2\psi \quad (5)$$

where ρ is the surface density. Note that this expression differs by a factor of $\sqrt{5}$ from *Nimmo and Pappalardo* [2006] because of an incorrect spherical harmonic normalization in the latter paper. Equation (5) assumes that there are no other gravity anomalies present (e.g., a compensating mantle plug), which is reasonable for icy satellites where the silicate mantle is typically at several hundred km depth. The gravitational perturbation thus depends on the depth and angular size of the impact basin, as expected.

[11] For simplicity, we have neglected the effect of the ejecta blanket and any central peak. The latter is unlikely to have a significant effect, as its mass is small compared with the total mass removed. The ejecta blanket, however, can reduce the effective potential anomaly, by a factor of $\approx$5 [*Melosh*, 1975] if the blanket extends uniformly out to two basin radii and no material escapes the satellite. Scaling arguments [*Veverka et al.*, 1986] suggest that most ejecta is retained; however, the distribution of ejecta is hard to infer from Voyager-era data [*Moore et al.*, 2004] and the quantity of material vapourized and thus permanently lost is unknown. Imaging by the Cassini spacecraft is likely to make the role of the ejecta clearer.

[12] Given the present-day location of the basin (θ_L^f, ϕ_L^f) and an estimate of the load size (parameterized by Q), equations (1)–(3) may be used to infer the reorientation caused by the basin. To do so, we need to calculate the Love numbers k_f^T* and k_f^T. These will depend on the density and (for k_f^T) rigidity structures of the satellites, which are not in general well known. We will therefore make the conservative assumption that $k_f^T* = 1.5$, the value for a homogeneous fluid body, and that $k_f^T = 0$ (perfectly rigid). More complicated approaches which involve calculating the load Love number are possible, but require the original basin depth and satellite internal structure to be known. The simple approach adopted here ensures that our estimate of the reorientation angle θ_R will be conservative.

3. Observations

[13] Table 1 summarizes the location, diameter D and present-day maximum depth $d_{\max}$ of the impact basins we consider [*Moore et al.*, 2004]. To be conservative, depth is defined as below the background elevation, rather than relative to the crater rim. Topographic profiles across these impact basins [*Moore et al.*, 2004] suggest that they are generally flat-floored, and thus that our assumption of a constant-depth basin is reasonable. We therefore assume that $h = d_{\max}$. If the crater had a parabolic shape, rather than a flat floor, then the effective value of h would be $d_{\max}/2$.

[14] The initial basin depth, which would have been significantly greater than that observed now, was used in the calculations of *Melosh* [1975] and *Murchie and Head* [1986]. We instead use the present-day depth partly to be conservative, and partly because the remaining present-day depression is likely to be elastically supported, and will thus give rise to a negative potential anomaly as assumed (equation (5)).

[15] For the Saturnian system, Enceladus appears to have no large impact basins [*Porco et al.*, 2006] and the reorientation of Iapetus was presumably dominated by its equatorial ridge [*Porco et al.*, 2005]. In the Uranian system, the only satellite which has convincingly-imaged impact basins is Titania [*Moore et al.*, 2004]. Although Io and Europa lack large impact basins, both Ganymede and Callisto possess enormous multi-ring structures [*Spudis*, 1993]. However, at least for Ganymede, the topography of these structures appears to be very flat [*Schenk*, 1998], probably as a result of relaxation subsequent to impact formation. We will therefore neglect these satellites in this study. Triton does not appear to possess any unambiguous impact basins [*Smith et*

Table 1. Impact Basins[a]

Body/ Basin	R, km	P, days	Colat. θ_L^f	E. Lon., ϕ_L^f	D, km	d_{max}, km	ψ	Q	Δg, mGal	$J_2^L/J_{2,hyd}$	ϕ_R	θ_R	σ, MPa
Mimas Herschel	196	0.942	87°	−111°	135	11	19.7°	−0.38	−5.7	0.152	86.2°	1.1°	0.44
Tethys Odysseus	530	1.888	60°	−130°	450	3	24.3°	−0.22	−5.9	0.089	79.1°	4.2°	0.50
Dione Aeneas	560	2.737	64°	−46°	175	3	9.0°	−0.07	−0.9	0.027	103.3°	1.1°	0.05
Rhea Tirawa	764	4.518	54°	−150°	350	5	13.1°	−0.48	−3.9	0.190	67.0°	6.7°	0.12
Titania Gertrude	790	8.706	107°	−68°	400	2	14.5°	−0.83	−1.9	0.333	−88.1°	12.3°	0.04
Pluto	1152	6.38	(45°)	(−90°)	(602)	(2)	(15°)	(−0.33)	(−2.3)	(0.129)	(90.0°)	(9.5°)	(0.05)
Charon	593	6.38	(45°)	(−90°)	(310)	(2)	(15°)	(−0.63)	(−1.8)	(0.253)	(90.0°)	(19.7°)	(0.10)

[a]Here R and P are the satellite radius and period, D and d_{max} are the basin diameter and maximum depth [from *Moore et al.*, 2004], Q is the dimensionless load (equation (4)), θ_R is the amount of poleward reorientation, ϕ_R is the longitude of the initial rotation axis, Δg is the degree-2 gravity anomaly at 100 km spacecraft altitude, calculated from $G_{20}{}^{IL}$ using the method given by *Nimmo and Pappalardo* [2006], ψ is the basin angular radius and σ is the approximate reorientation stress given by equation (6) using $p = 1$, $h_f^T = 2.5$, $\nu = 0.3$ and $\mu = 4$ GPa. The quantity $J_2^L/J_{2,hyd}$ is the ratio of the potential anomaly due to the impact basin compared to that expected for a rotating hydrostatic body, calculated using equation (8) with $k_f^T* = 1.5$. Satellite data obtained from *Lodders and Fegley* [1998] except for densities of Saturnian satellites [*Thomas et al.*, 2007] and we assumed $\rho = 900$ kg m^{-3}. It is not known whether Pluto and Charon have any impact basins; the calculations presented here represent an example assuming the basin dimensions are comparable to those of the other icy satellites.

al., 1989], and the Pluto/Charon system has not yet been imaged by spacecraft.

4. Results

[16] Figure 1 shows the polewards reorientation angle θ_R as a function of basin angular radius ψ and the centripetal acceleration at the surface of the satellite. The basin depth (2 km) and final colatitude ($\theta_L^f = 45°$) are kept constant, and we are assuming reorientation along the meridian perpendicular to the tidal axis. As expected, larger basins lead to greater reorientation. Similarly, other things being equal, a satellite which is spinning faster experiences less reorientation, because the equatorial and tidal bulges are larger.

[17] Table 1 tabulates the polewards reorientation θ_R expected for the real basin locations and depths. Herschel, because it is equatorial, produces almost no reorientation, despite its relatively large perturbation to the gravity field. Aeneas, being both shallow and relatively small, likewise produces little reorientation. Odysseus and Tirawa result in larger (4.2° and 6.7°, respectively) reorientations - the former because Odysseus is large, and the latter because Rhea is a slow rotator. Gertrude results in a polewards reorientation of 12.3° from a nearly equatorial initial location. Although the gravity anomaly of Gertrude is smaller than that of Tirawa, the reorientation is larger because of Titania's slower rotation compared to Rhea.

5. Consequences of Reorientation

[18] Apart from the effect of an ejecta blanket, which is hard to quantify, the results presented in Table 1 will tend to underestimate the actual amount of reorientation. We have used the present-day basin depth because the reorientation timescale is likely to scale with, and be longer than, the basin relaxation timescale [*Tsai and Stevenson*, 2007]. However, if the basin width significantly exceeds the depth of the layer in which relaxation occurs, the relaxation timescales can grow very large [*Melosh*, 1989], in which case the present-day basin depth will underestimate the relevant value.

[19] Table 1 shows that the presence of impact basins can lead to significant reorientation of these bodies. As with Enceladus [*Nimmo and Pappalardo*, 2006], such reorientation is likely to have observable consequences. Perhaps most importantly, reorientation will lead to stresses sufficient to cause fractures, and probably a global pattern of tectonic features [*Melosh*, 1980]. The approximate size of the stresses may be derived as follows. Following *Leith and McKinnon* [1996] the stress due to a reorientation angle θ_R is given by

$$\sigma = p f \mu \left(\frac{1+\nu}{5+\nu}\right) \sin\theta_R \tag{6}$$

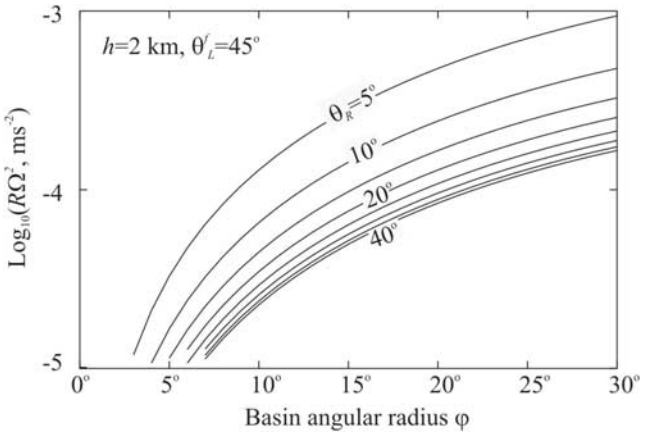

Figure 1. Polewards reorientation angle θ_R (plotted at 5° intervals) as a function of basin angular width ψ and satellite centripetal acceleration $R\Omega^2$, calculated using equations (1)–(5). Basin depth h = 2 km, initial colatitude $\theta_L^f = 45°$; reorientation is assumed to take place around the tidal axis (see text).

where μ is the shear modulus, ν is Poisson's ratio, f is the flattening, p is a factor of order unity which depends on the location of the point in question and here it has been assumed that θ_R is a small angle. For reorientations of the kind considered here, the relevant flattening is that which occurs perpendicular to the tidal axis. From *Dermott and Thomas* [1988] we have

$$f = \frac{1}{2}\frac{R^3\Omega^2}{GM}h_f^T \quad (7)$$

where h_f^T is the degree-two tidal h Love number which has a value of 2.5 for a homogeneous, hydrostatic body. Equations (6) and (7) may be combined to derive the approximate magnitude of the stress generated by reorientation. These stresses are tabulated in Table 1 assuming that $h_f^T = 2.5$ (hydrostatic) and $p = 1$. Under these assumptions, reorientation stresses in excess of 0.1 MPa (comparable to diurnal tidal stresses on Europa) can be generated, and are likely to generate detectable tectonic features. Mimas and Tethys experience the largest stresses, despite the relatively small reorientations, because these bodies have the shortest periods and thus the largest flattening (equation (7)). However, bodies which are more rigid will have a smaller flattening ($h_f^T < 2.5$) and thus experience lower stresses.

[20] Another consequence of reorientation is that the expected apex-antapex asymmetry in impact crater distribution [*Zahnle et al.*, 2001] will be smeared out [e.g., *Plescia*, 1988]. Finally, the present-day impact basins (assuming an uncompensated state) are predicted to generate negative degree-two gravity anomalies, tabulated in Table 1, of order a few mGal at 100 km altitude, which may be detectable with sufficiently close spacecraft flybys [cf. *Palguta et al.*, 2006].

[21] These gravity anomalies are not negligible compared to those expected from the rotational and tidal deformation of a fluid body. For a synchronous hydrostatic rotator the polar degree-2 gravity coefficient is given by $J_{2,hyd} = (5\Omega^2 R^3/6GM)k_f^T*$ where k_f^T* is the degree-two fluid Love number [*Hubbard and Anderson*, 1978]. It may be shown that the degree-two contribution from a polar basin, J_2^L is given by $-\sqrt{5}G_{20}{}^{L}$. Making use of equation (5) and neglecting the minus sign, the ratio of the degree-2 gravity coefficient due to the basin to the degree-2 coefficient expected for a fluid (hydrostatic) rotating body is given by

$$\frac{J_2^L}{J_{2,hyd}} = \frac{6\pi}{5}\frac{h\rho G}{\Omega^2 R k_f^T*}\cos\psi\sin^2\psi. \quad (8)$$

[22] Table 1 tabulates the size of this ratio and demonstrates that the potential coefficients due to an impact basin can be up to one-third of those expected for a hydrostatic body. Thus, determination of satellite structure using measured values of J_2 and/or C_{22} and the hydrostatic assumption [e.g., *Anderson et al.*, 2001] may result in inaccurate conclusions if the present-day basins are indeed uncompensated.

[23] Slow-rotating bodies undergo transient wobble during reorientation. The wobble amplitude is controlled by the rotation number *Ro* given by *Spada et al.* [1996, equation 2]. If the relaxation time is given by $\eta/\rho gR$, where η is the viscosity and g the acceleration due to gravity, then we obtain

$$Ro \approx 160\left(\frac{\Omega}{10^{-4}\ \mathrm{rad\ s^{-1}}}\right)^3\left(\frac{\eta}{10^{15}\ \mathrm{Pa\ s}}\right)\cdot\left(\frac{2000\ \mathrm{kg\ m^{-3}}}{\rho}\right)\left(\frac{0.1\ \mathrm{m\ s^{-2}}}{g}\right)^2 \quad (9)$$

where we have assumed a Love number of 1.5.

[24] For $Ro \ll 1$ wobbles with decaying amplitude will be superimposed on the background polar wander. Thus, slow-rotating icy satellites may demonstrate transient wobble during reorientation. However, the results obtained here assume a low viscosity characteristic of ice near the melting temperature, which may not be applicable to cold or more silicate-rich bodies. Furthermore, the analysis of *Spada et al.* [1996] neglects the effect of a stabilizing fossil bulge. Thus, whether transient wobble is likely have occurred is not yet clear and should be the focus of future work.

6. Discussion and Conclusions

[25] Our main conclusion is that, particularly for slow-rotating satellites, impact basins are likely to have led to significant reorientations, possibly accompanied by transient wobble. Apart from the (uncertain) effect of the ejecta blanket, the reorientation magnitudes we derive are likely to be conservatively small. Although the reorientations are largest for slow-rotating bodies (e.g., Titania), the resulting stresses are larger for more rapid rotators (e.g., Tethys). The resulting gravity anomalies are likely to be detectable with spacecraft flybys, and may also contaminate inferences of satellite interior structures based on the hydrostatic assumption.

[26] More speculatively, the observation that Herschel is almost exactly at the equator is somewhat surprising (*Moore et al.* [2004] and *Greeley and Batson* [1997] give $\theta_L{}^f = 90°$ and 87°, respectively). If impacts were spatially isotropic in latitude, an impact within ±3° of the equator has a probability of about 5%. An alternative possibility is that Mimas actually reoriented towards the equator, implying it was associated with a mass excess. Some lunar craters apparently possessed such a mass excess before being flooded with lavas [*Wieczorek and Phillips*, 1999], presumably as a result of the immediate post-impact rebound process. Later flooding of Herschel by cryovolcanism could also account for a mass excess, but is not supported by available imagery [*Moore et al.*, 2004]. In either event, a mass excess implies a positive gravity anomaly, which is potentially detectable by Cassini.

[27] Finally, Pluto and Charon are both slow rotators and thus prone to reorientation. Although no impact features are currently known, it is likely that both bodies possess basins of comparable sizes to those listed in Table 1. Taking $\psi = 15°$ and using basin parameters similar to those in Figure 1, the reorientation angles for Pluto and Charon are 9.5° and 19.7°, respectively. Charon reorients further than Pluto because the effective load increases as the satellite radius decreases (equations (4) and (5)). Thus, if Pluto or Charon possess impact basins comparable to those examined here, significant reorientation is very likely to have occurred.

[28] **Acknowledgments.** The authors thank M. Greff-Lefftz and an anonymous reviewer for helpful comments. This work was supported by NASA Outer Planets Research and the Carnegie Institution of Washington.

References

Anderson, J. D., R. A. Jacobson, T. P. McElrath, W. B. Moore, and G. Schubert (2001), Shape, mean radius, gravity field and interior structure of Callisto, *Icarus*, *153*, 157–161.

Dermott, S. F., and P. C. Thomas (1988), The shape and internal structure of Mimas, *Icarus*, *73*, 26–65.

Gold, T. (1955), Instability of the Earth's axis of rotation, *Nature*, *175*, 526–529.

Greeley, R., and R. Batson (1997), in *The NASA Atlas of the Solar System*, Cambridge Univ. Press, Cambridge, U. K.

Hubbard, W. B., and J. D. Anderson (1978), Possible flyby measurements of Galilean satellite interior structure, *Icarus*, *33*, 336–341.

Janes, D., and H. Melosh (1988), Sinker tectonics—An approach to the surface of Miranda, *J. Geophys. Res.*, *93*, 3127–3143.

Kirschvink, J., R. Ripperdan, and D. Evans (1997), Evidence for large-scale reorganization of early Cambrian continental masses by inertial interchange true polar wander, *Science*, *277*, 541–545.

Leith, A. C., and W. B. McKinnon (1996), Is there evidence for polar wander on Europa?, *Icarus*, *120*, 387–398.

Lodders, K., and B. Fegley (1998), *The Planetary Scientist's Companion*, Oxford Univ. Press, New York.

Matsuyama, I., J. X. Mitrovica, M. Manga, J. T. Perron, and M. A. Richards (2006), Rotational stability of dynamic planets with elastic lithospheres, *J. Geophys. Res.*, *111*, E02003, doi:10.1029/2005JE002447.

Melosh, H. J. (1975), Large impacts and the Moon's orientation, *Earth Planet. Sci. Lett.*, *26*, 353–360.

Melosh, H. J. (1980), Tectonic patterns on a reoriented planet: Mars, *Icarus*, *44*, 745–751.

Melosh, H. J. (1989), *Impact Cratering: A Geologic Process*, Oxford Univ. Press, New York.

Moore, J., P. Schenk, L. Bruesch, E. Asphaug, and W. McKinnon (2004), Large impact features on middle-sized icy satellites, *Icarus*, *171*, 421–443.

Murchie, S., and J. Head (1986), Global reorientation and its effect on tectonic patterns on Ganymede, *Geophys. Res. Lett.*, *13*, 345–348.

Nimmo, F., and R. T. Pappalardo (2006), Diapir-induced reorientation of Saturn's moon Enceladus, *Nature*, *441*, 614–616.

Ojakangas, G. W., and D. J. Stevenson (1989), Polar wander of an ice shell on Europa, *Icarus*, *81*, 242–270.

Palguta, J., J. D. Anderson, G. Schubert, and W. B. Moore (2006), Mass anomalies on Ganymede, *Icarus*, *180*, 428–441.

Plescia, J. (1988), Cratering history of Miranda—Implications for geologic processes, *Icarus*, *73*, 442–461.

Porco, C. C., et al. (2005), Cassini Imaging Science: Initial results on Phoebe and Iapetus, *Science*, *307*, 1237–1242.

Porco, C., et al. (2006), Cassini observes the active south pole of Enceladus, *Science*, *311*, 1393–1401.

Rubincam, D. (2003), Polar wander on Triton and Pluto due to volatile migration, *Icarus*, *163*, 469–478.

Schenk, P .M. (1998), Geology of Gilgamesh, Ganymede: New insights from stereo and topographic mapping, *Lunar Planet. Sci.* [CD-ROM], XXIX, abstract 1949.

Smith, B., et al. (1989), Voyager-2 at Neptune—Imaging science results, *Science*, *246*, 1422–1449.

Spada, G., R. Sabadini, and E. Boschi (1996), Long-term rotation and mantle dynamics of the Earth,Mars and Venus, *J. Geophys. Res.*, *101*, 2253–2266.

Spudis, P. (1993), *The Geology of Multi-ring Impact Basins*, Cambridge Univ. Press, Cambridge.

Thomas, P. C., et al. (2007), Shapes of the Saturnian icy satellites and their significance, *Icarus*, in press.

Tsai, V. C., and D. J. Stevenson (2007), Theoretical constraints on true polar wander, *J. Geophys. Res.*, *112*, B05415, doi:10.1029/2005JB003923.

Veverka, J., P. Thomas, T. V. Johnson, D. Matson, and K. Housen (1986), The physical characteristics of satellite surfaces, in *Satellites*, edited by J. Burns and M. Matthews, pp. 342–402, Univ. of Arizona Press, Tucson.

Wieczorek, M., and R. J. Phillips (1999), Lunar multiring basins and the cratering process, *Icarus*, *139*, 246–259.

Willemann, R. (1984), Reorientation of planets with elastic lithospheres, *Icarus*, *60*, 701–709.

Zahnle, K., P. Schenk, S. Sobieszczyk, L. Dones, and H. F. Levison (2001), Differential cratering of synchronously rotating satellites by ecliptic comets, *Icarus*, *153*, 111–129.

I. Matsuyama, Department of Terrestrial Magnetism, Carnegie Institution of Washington, Washington, DC 20015–1305, USA. (matsuyama@dtm.ciw.edu)

F. Nimmo, Department of Earth and Planetary Sciences, University of California, Santa Cruz, 1156 High Street, Santa Cruz, CA 95064, USA. (fnimmo@es.ucsc.edu)